Mountain Peatlands and Drought: Carbon Cycling in the Pyrenees Amidst Global Climate Change

Raphaël Garisoain, Adrien Jacotot, Christine Delire, Stéphane Binet, Gael Le Roux, Simon Gascoin, Thomas Rosset, Sébastien Gogo, Franck Granouillac, Virginie Payre-Suc, et al.

JGR Biogeosciences

RESEARCH ARTICLE
10.1029/2024JG008041

Mountain Peatlands and Drought: Carbon Cycling in the Pyrenees Amidst Global Climate Change

Raphael Garisoain[1,2], Adrien Jacotot[3,4], Christine Delire[1], Stéphane Binet[5], Gael Le Roux[2], Simon Gascoin[6], Thomas Rosset[2], Sébastien Gogo[7], Franck Granouillac[2], Virginie Payre-Suc[2], and Laure Gandois[2]

[1]CNRM, Meteo-France, CNRS, Universite de Toulouse, Toulouse, France, [2]CRBE, Université de Toulouse, CNRS, Toulouse, France, [3]Institut National de la Recherche en Agriculture, Alimentation et Environnement (INRAE), UMR 1069 SAS, Rennes, France, [4]Institut des Sciences de la Terre d'Orléans (ISTO), Université d'Orléans, UMR7327, CNRS, Orléans, France, [5]Agence de l'eau Adour Garonne, Toulouse, France, [6]Centre d'Etudes Spatiales de la BIOsphère, Université de Toulouse, CNRS, CNES, IRD, INRA, Toulouse, France, [7]UMR-CNRS 6553 ECOBIO, Université de Rennes, Rennes, France

Key Points:

- Investigation of the carbon balance of a mountain peatland by integrating carbon flux measurements, satellite imagery, statistical models
- Annual carbon balances were highly variable and the peatland acted as a source of carbon on average over the period
- A large carbon loss occurred during the extreme drought

Supporting Information:

Supporting Information may be found in the online version of this article.

Correspondence to:

L. Gandois,
Laure.gandois@toulouse-inp.fr

Citation:

Garisoain, R., Jacotot, A., Delire, C., Binet, S., Le Roux, G., Gascoin, S., et al. (2024). Mountain peatlands and drought: Carbon cycling in the Pyrenees amidst global climate change. *Journal of Geophysical Research: Biogeosciences*, *129*, e2024JG008041. https://doi.org/10.1029/2024JG008041

Received 25 JAN 2024
Accepted 14 JUN 2024

Abstract This study provides a multi-year (2017–2022) Net Ecosystem Carbon Balance (NECB) of a Pyrenean mountainous peatland through the integration of field data, satellite imagery, and statistical modeling. Fluvial organic carbon export was measured at 30 min frequency, while gaseous (CO_2 and CH_4) exchanges were measured monthly using closed chambers. These measurements were combined with Sentinel-2 derived chlorophyll index and in situ high frequency (1 hr) measurements of key environmental variables such as air temperature, photosynthetically active radiation, and water table level, to develop hourly gaseous carbon flux models ($R^2 = 0.69$ for GPP, $R^2 = 0.84$ for ER, $R^2 = 0.59$ for CH_4). Over the 2017–2022 period, modeled average GPP (610 ± 39 gC.m^{-2}.year^{-1}) and ER (641 ± 59 gC.m^{-2}.year^{-1}) showed that the peatland acted as a weak source of CO_2 to the atmosphere, releasing 31 ± 73 gC.m^{-2}.year^{-1}. Considering fluvial carbon export and CH_4 exchanges, the loss of carbon from the peatland increased to 55 ± 73 gC.m^{-2}.year^{-1}. Dissolved organic carbon constituted 8%–106% of the NECB. The estimated long-term organic accumulation rate indicated a steady carbon accumulation rate of 16.4 gC.m^{-2}.year^{-1}, contrasting with the contemporary NECB, suggesting a recent shift in ecosystem functioning from a carbon sink to a source. The study underscores the role of water availability and air temperature through a drought index (DI), in shaping the NECB. The DI correlated significantly with annual carbon gaseous fluxes, except for 2022, marked by an intense drought. During this year the peatland became a large source of carbon (189 gC.m^{-2}.year^{-1}) to the atmosphere.

Plain Language Summary Peatlands contain large amounts of organic carbon that was accumulated during the Holocene. Mountain peatlands, although very numerous, are still poorly known because they are small and scattered in the landscape in valley bottoms often difficult to reach. Whether these systems currently accumulate carbon and may continue to do so in the future is largely unknown. Here we present a comprehensive assessment of the carbon balance of a mountain peatland in the French Pyrenees, based on field measurements including winter CH_4 fluxes and fluvial export of dissolved organic carbon, satellite imagery and statistical models. We show that on average over 2017–2022 the peatland acted as a weak source of carbon to the atmosphere and also lost carbon to the nearby stream. However, this weak source hides strong interannual variability: in 2018 the peatland acted as a carbon sink but in the year 2022 when an intense drought struck SW Europe, the peatland acted as a substantial source of carbon. Our study underscores the vulnerability of mountain peatlands to climatic fluctuations, emphasizing the necessity for comprehensive monitoring and modeling approaches to accurately assess their carbon balance under changing climatic conditions, including extreme events.

1. Introduction

Peatlands are central to the global carbon cycle (Gorham et al., 2012; Harenda et al., 2018; Parish et al., 2007). These huge carbon stock result from an unbalanced carbon budget over millennia (Loisel et al., 2017; Nugent et al., 2018). In peatlands, carbon inputs by primary productivity exceeds carbon losses in forms of CO_2 and CH_4 emissions to the atmosphere and fluvial carbon export (Abdalla et al., 2016; Billett et al., 2010; M. R. Turetsky et al., 2014), leading to negative NECB (Net Ecosystem carbon Balance, (Chapin et al., 2006)). Waterlogged

conditions restrict oxygen to the topmost centimeters of the peat, limiting aerobic organic matter degradation emitting CO_2, but promoting methanogenesis. Then, peatlands constitute a large but underconstrained source of CH_4 to the atmosphere (Kirschke et al., 2013). Peatlands are also recognized as potentially important sources of organic carbon to surface waters, at local (Rosset et al., 2019; Tunaley et al., 2017) and global scales (Rosset et al., 2022). If undisturbed peatlands have remained carbon sinks over millennia, It has been widely demonstrated that carbon uptake by peatlands is considerably reduced when disturbed (Fenner & Freeman, 2011; M. Turetsky et al., 2002). Global changes and drought events can potentially alter the carbon balance of peatlands, turning them from carbon sinks to sources (Carter et al., 2012; Keane et al., 2021; Loisel et al., 2021; Page & Baird, 2016; Yan et al., 2022). This hypothesis is still debated due to a lack of comprehensive field observations (Muhr et al., 2011; Wang et al., 2015).

Climate change is expected to be particularly pronounced at high elevation, with direct impacts on mountain ecosystems (Rogora et al., 2018). At the scale of the Pyrenean range, recent downscaling projections predict a temperature increase for the next century, and if the precipitation amount variation is not clear, soil moisture might be reduced in relation to higher evapotranspiration (Amblar-Frances et al., 2020). Similarly, the snow season will be shortened due to the temperature increase. Klos et al. (2023) have shown that snow deficit in winter and drought lead to reduced soil surface saturation in a wetland area under a Mediterranean climate. Therefore, a strong impact on the carbon cycling within mountainous peatlands of the Pyrenees is expected.

The exceptional weather during summer and fall of 2022 in Western Europe might be a good example of such future disruption. July was the hottest on record in Spain since the 1970ies, and summer temperatures were on average 3°C higher than climatological values over large parts of S-W Europe (Serrano-Notivoli et al., 2023). Close to 30% of Europe was under severe summer drought (van der Woude et al., 2023). The flow of the Po River reached its lowest point in the last two centuries (Montanari et al., 2023). This unprecedented summer heat led to a general reduced carbon uptake by European forests (van der Woude et al., 2023) and a decreased greenness of the above tree-line ecosystems in the Alps (Choler, 2023).

While many studies focused on carbon dynamic in northern peatlands (Abdalla et al., 2016; M. R. Turetsky et al., 2014; Yu, 2012), there is still a great lack of measurement data on mountain peatlands, which are less accessible. Many mountain peatlands are still unknown and are not yet included in global peat maps (Xu et al., 2018). Their role in the local and global carbon cycles remains uncertain. Indeed, the few existing studies highlight their sensitivity to climate change (Fonseca et al., 2023), related to the specific ecological and hydrological condition shaping carbon cycling in these ecosystems (Millar et al., 2017; Pullens et al., 2016; Santoni et al., 2023; Yao et al., 2022). These include a short vegetation period, important carbon emissions during non-vegetation period (Pullens et al., 2016; Yao et al., 2022), the influence of altitude on ecosystem functioning (Millar et al., 2017), a strong inter-annual variability of carbon balance due to climate variability experienced by alpine peatlands (Pullens et al., 2016), or the major role of storm events in fluvial carbon export (Birkel et al., 2017; Rosset et al., 2019).

Investigating the role of climatic drivers on individual carbon fluxes and ultimately on peatlands NECB requires establishing pluri-annual inventories of carbon fluxes. Such studies are scarce (D'Angelo et al., 2021; Dinsmore et al., 2010; Nugent et al., 2018; Roulet et al., 2007). More studies have established multiannual evolution of NEE (Aurela et al., 2007; McDonald et al., 2023; Nugent et al., 2018), with most studies being limited to the vegetation period. Multiannual studies allow identifying drivers for annual and seasonal fluxes, highlighting the role of all the components of the peatland C cycle, NEE, CH_4 fluxes and DOC exports (Roulet et al., 2007).

In this context, this study aims at quantifying the NECB (CO_2, CH_4 exchange and fluvial carbon export) in a mountain peatland located within the French Pyrenees over a six-year period (2017–2022). This study period includes the major drought event which occurred during the 2022 summer (Faranda et al., 2023). Our main objectives are to (a) model high-frequency CO_2 and CH_4 fluxes using monthly in situ chamber fluxes measurements combined with environmental variables monitored on-site and derived from satellite observations, (b) quantify the peatland's inter-annual NECB including the drought event, (c) identify the influence of the drought event on the components of the peatland C balance (CO_2 and CH_4 fluxes, DOC exports).

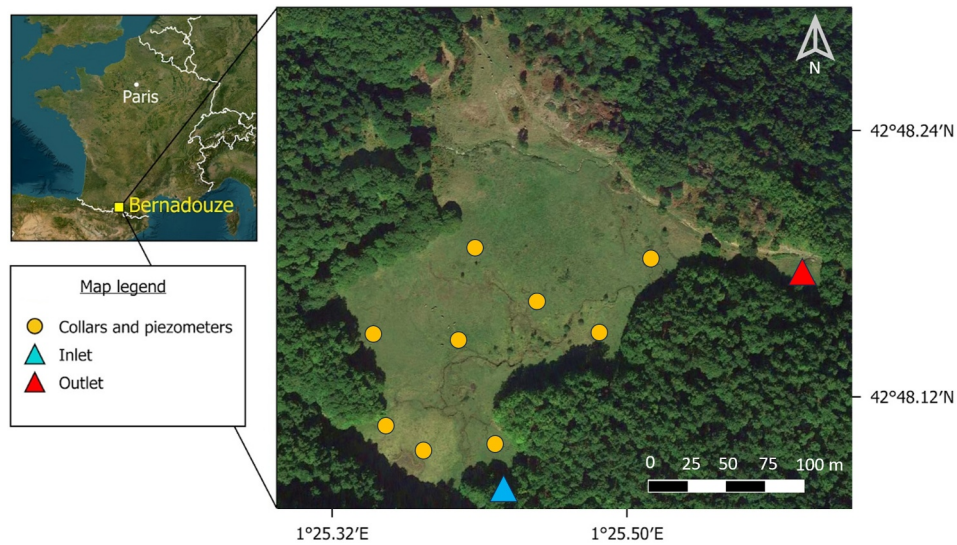

Figure 1. Map of the peatland of Bernadouze, in the Pyrenees (France). The yellow circles indicate the locations of the soil collars for GHG (greenhouse gas) flux measurements and of the automatic piezometers. The blue and red triangles indicate respectively the peatland inlet and outlet where dissolved organic matter fluorescence (fDOM) is measured in situ at a high frequency (30 min).

2. Materials and Methods

2.1. Study Site Description

Field work was conducted in the peatland of Bernadouze, a French mid-altitudinal north-facing peatland (N42° 48'10.4″, E01°25'26.1″; 1,343m asl) located in the Pyrenees mountains (Figure 1). This peatland, classified as a regional biological reserve since 1983 and a Natura 2000 site since 2007, is one of the four sites of the French National Peatland Observatory Service SNO-Tourbieres (Gogo et al., 2021). The peatland has developed for 5,000 years (Jalut et al., 1982) in a 1.4 km watershed with very steep slopes (50% on average). It covers an area of 4.7 ha, has an average depth of 2m, with some areas down to 9.5 m (Jalut et al., 1982; Reille, 1990). Its size and altitude are representative of peatlands in the East part of the Pyrenees. Vegetation characteristic of an ombrotophic area (*Sphagnum palustre* and *Sphagnum capillifolium*) and a minerotrophic area (herbaceous *Carex demissa* and *Equisetum fluviatile*) are both present on the site (Garisoain et al., 2023; Henry et al., 2014) see Figure S1 in Supporting Information S1. The climate is temperate with a strong continental influence, classified "Cfb" following Koppen-Geiger typology (Rubel et al., 2017). Mean annual temperatures and precipitation over the 1959–2022 period ranged around 7.5°C and 1,478 mm.year^{-1}, respectively (Rosset et al., 2019; Vernay et al., 2022; Vidal et al., 2010). The peatland is usually covered with snow from November to March.

2.2. Environmental Monitoring

Air temperature (AT) and photosynthetically active radiation (PAR, SKP215 sensor, Campbell Scientific) were measured directly in the peatland, precipitation (P) at a weather station located ~450m away (https://osr.cesbio.cnrs.fr/sites-dobservation-donnees/sites-perennes/bernadouze/), and water table depth (WTD) by 9 automatic piezometer probes (Orpheus Mini water level logger) (Figure 1). Piezometer wells are 50 mm diameter PVC tubes. All data were recorded at a 1-hr frequency. In the remainder of the study, the WTD refers to the mean value obtained from the 9 piezometers. AT and PAR sensors occasionally experienced disruptions due to periodic snowfall and battery losses, resulting in gaps in the time series. To overcome these gaps, AT and PAR derived from the S2M reanalysis was used, which combines the French weather service SAFRAN meteorological reanalysis (8 km resolution) with the SURFEX/ISBA-crocus snow cover model (Vernay et al., 2022). The S2M chain was applied in a local mode, that is, at the scale of the "Couserans" massif, assuming homogeneous weather conditions across the massif for equivalent altitudes but accounting for local topographic mask in the calculation of the shortwave radiation. The vertical resolution of the S2M model is 300 m, with an hourly frequency. Particularly for PAR, the site's topographical features were carefully considered, through altitude, slope, and

aspect of the peatland. The S2M chain provided a time series from 2013 to 2022 corresponding to both direct and diffuse incident solar energy. We used a linear regression between the measured PAR radiation in the field and the total incident radiation from S2M to validate the PAR time series. Lastly, start and end dates of snow cover over the peatland were identified based on S2M snowfall records and Sentinel-2 image screening (Sentinel-hub Playground, https://apps.sentinel-hub.com/sentinelplayground/), respectively. The CI (chlorophyll index) vegetation index is commonly used as a proxy for the photosynthetic activity of vegetation. CI was calculated from Sentinel-2 level 2A products, that is, bottom of atmosphere reflectances at a 20m resolution available in Google Earth Engine (S2 SR HARMONIZED data set). The CI index was spatially averaged over the ombrotrophic zone of the peatland, where *Sphagnum* mosses predominate (Garisoain et al., 2023).

2.3. Development of an Annual Drought Index Based on AT and WTD

A Drought Index (DI) was developed (a) to evaluate the drought pressure on the site, combining temperature and water level, and (b) to compare the interannual variability of cumulated carbon fluxes to the combined variations of AT and WTD, the two main variables available for the site that influence these fluxes, analogous to ombrothermic diagrams. The index is defined as the total area above zero and below the curve resulting from the subtraction of hourly $WTD_{normalized}$ from $AT_{normalized}$ time series (Figure S4 in Supporting Information S1), after data normalization.

2.4. Monthly Monitoring of CO_2 and CH_4 Fluxes

Monitoring of CO_2 and CH_4 exchanges between the peatland and the atmosphere started in 2017 for CO_2 and 2019 for CH_4 and was performed using the static chamber technique (with the use of custom-made transparent acrylic chambers, 30 cm in diameter and height placed on 30 cm diameter soil-collars). This strategy was adopted in 2016 since installation of an eddy covariance tower was impossible due to the modest size and topography (strong slopes) of the site. Collars were inserted in 9 locations close to the automatic piezometers, and spatially distributed to cover the vegetation mosaic (Figure 1). Despite the recognized potential for soil collars-induced biases in gas flux measurements (Heinemeyer et al., 2011; Jovani-Sancho et al., 2017; Ramirez et al., 2017), this approach is the sole method that could guarantee a perfect seal between the chamber and the peatland soil, featuring uneven microtopography and densely packed vegetation. Monthly measurements were conducted mostly during snow-free periods, resulting in 50 and 34 campaigns for CO_2 and CH_4, respectively. In each campaign, flux measurements were performed on five randomly selected collars, following the recommendation of ICOS network (Pavelka et al., 2018). Flux measurements at each selected location were taken around mid-day, first in day-light using the transparent chamber, yielding the net ecosystem exchange (NEE). The chamber was subsequently covered with an opaque aluminum cover to quantify the ecosystem respiration (ER). Each flux measurement lasted 5 min. The measurements over the 5 plots lasted for less than 2 hr. The chamber has an automatic fan. The evolution of CO_2 concentrations in the chamber was monitored with a CARBOCAP® GMP 343 CO_2 probe (VAISALA) from 2017 to 2021, and to a LI-7810 (LI-COR) analyzer from 2019 to 2022. From 2019 to 2022, concurrent monitoring was performed to confirm the similarity of the measurements from the two analyzers (Figure S2 in Supporting Information S1). For CH_4, all measurements were conducted with the LI-7810 since 2019. Flux measurements were carried out during the winter of 2021 and 2022. The chamber was positioned directly on the snow, because the collars were buried under 0.5–1 m snow. Additionally, manual measurements of AT, PAR and WTD were also conducted with each flux measurement.

Fluxes of CO_2 and CH_4 were then calculated from the linear regression of the concentrations inside the chamber over time, using the following equation:

$$F_{CO_2,CH_4} = \frac{d_{CO_2,CH_4}}{dt} \times \frac{h \times Pa}{R \times AT} \quad (1)$$

where F is the flux of CO_2 or CH_4 ($\mu mol.m^{-2}.s^{-1}$), $\frac{d_{CO_2,CH_4}}{dt}$ the slope of the evolution in gas concentrations within the chamber as a function of time ($ppm.s^{-1}$); h the total headspace height (chamber + soil collar; m); Pa the atmospheric pressure ($J\ m^{-3}$); R the ideal gas constant of 8.314 ($J.K^{-1}.mol^{-1}$); and AT the air temperature inside the chamber (K). Then, the gross primary productivity (GPP), was calculated as GPP = −NEE + ER.

Some collars were dominated by *Sphagnum* mosses, others by herbaceous vegetation or a mixture of the two. No significant differences in fluxes could be established when the collars were distinguished by dominant vegetation type (not shown see Supporting Information in Garisoain et al. (2023)). The fluxes considered below therefore correspond to the average over the entire peatland (*Sphagnum* mosses and herbaceous plants combined).

2.5. Modeling of Hourly GPP, ER, NEE, and CH_4

Hourly CO_2 and CH_4 fluxes across the studied period were determined for all combined plots, by fitting non-linear equations and empirical parameters to the in situ measurements and the auxiliary data collected during each campaign. First, the GPP was derived using PAR, AT and a chlorophyll index (CI) (Gitelson & Merzlyak, 1994). The CI index was obtained every 3–4 days from Sentinel-2 L2A data and was then linearly interpolated to daily values. This index has been demonstrated to be an effective predictor of CO_2 exchanges in peatlands (Tucker et al., 2022). The dependence on a near infrared vegetation index (the CI here) facilitates the representation of GPP seasonality (Junttila et al., 2021), while the reliance on hourly AT and PAR allows describing the diurnal cycles. The equation for GPP is as follows:

$$GPP = a \times PAR \times AT \times CI \tag{2}$$

here, GPP is in $\mu mol.m^{-2}.s^{-1}$, with PAR in $\mu mol.m^{-2}.s^{-1}$ and AT in K.

Then, ER was adapted from the equations of Bortoluzzi et al. (2006); Leroy et al. (2017), with the inclusion of GPP following Gao et al. (2015):

$$ER = \left(b \times \frac{WTD}{WTD_{\min}} + c\right) \times e^{d \times \frac{AT}{AT_{\max}}} + f \times GPP - g \tag{3}$$

with ER in $\mu mol.m^{-2}.s^{-1}$, WTD in m counted negative downward below ground and AT in K. WTD_{min} and AT_{max} represent the minimum and maximum values of WTD and AT observed throughout the study period, respectively.

The NEE ($\mu mol.m^{-2}.s^{-1}$) was then inferred from the calculated ER and GPP as follows:

$$NEE = ER - GPP \tag{4}$$

Lastly, CH_4 fluxes were estimated, from PAR, AT, CI, and WTD with the following equation:

$$FCH_4 = (h \times CI \times PAR + i \times CI \times AT + j \times AT) \times (l + m \times WTD) \tag{5}$$

here, FCH_4 is in $\mu mol.m^{-2}.s^{-1}$, PAR in $\mu mol.m^{-2}.s^{-1}$, AT in K, and WTD in m. WTD is negative when the water table lies beneath the soil surface.

Empirical parameters a, b, c, d, f, g, h, i, j, l, and m (Equations 2, 3, and 5) were determined through an optimization process ("curve fit" function) from the python scipy.optimize library that uses non-linear least squares to fit a function to the in situ GHG data. A function was fitted for each flux (GPP, ER, CH_4) or each Equations 2, 3, and 5. Specific values of the empirical parameters can be found in Table S1 in Supporting Information S1. Hourly time-series of GPP, ER, NEE, and FCH_4 were then computed using Equations 2–5 with the 1-hr frequency auxiliary data from S2M, the WTD recorded on the site, and the daily CI time-series. Finally, GPP was set to zero during snow-covered periods.

2.6. Fluvial Organic Carbon Export From the Peatland

The fluvial organic carbon export (DOC) from the peatland was determined following the methodology described in Rosset et al. (2019) The peatland area represents approximately 3% of the entire watershed. In order to ascertain the contribution of the peatland to the DOC flux (hereafter FDOC), a high frequency in situ protocol was developed at the inlet and outlet of the peatland (Figure 1). The DOC concentrations were estimated at a high temporal resolution (30 min) using an optical proxy (fluorescence of dissolved organic matter, fDOM) on a EXO-2 probe (YSI, USA), by following the signal correction and calibration described in Rosset et al. (2019). Inflow

and outflow DOC fluxes were determined, which enabled the calculation of the specific contribution of the peatland area to the watershed's DOC flux (from 64% to 85% of the outlet flux). High frequency temporal fluxes were finally summed annually to calculate the specific DOC flux in g $m^{-2}.yr^{-1}$.

2.7. Peat Core Sampling and Analysis

In September 2016, a one-m monolith was extracted using a stainless steel Wardenaar peat corer, in the south and ombrotrophic section (Rosset et al., 2020) of the peatland. The core was kept frozen and then sliced at a 1 cm resolution following the protocol described in De Vleeschouwer et al. (2010) and wet and dry mass were then determined for all subsamples to calculate the peat bulk density. Total carbon and nitrogen contents were analyzed for all samples using a Flask 20,000 elemental analyzer (ThermoScientific, USA). In order to establish carbon accumulation rates at different timescales, seven samples (averages depths of −1.5, −3.3, −5.4, −7.4, −13.6, −28.7 and −67.7 cm, Table S2 in Supporting Information S1), *Sphagnum* macro-fossils were extracted and sent to Beta Analytic (USA) for 14C measurements (acid/alkali/acid treatment). Five samples contained radiocarbon from aerial nuclear weapon tests ("so-called bomb 14C pulse"). Based on the 14C bomb-pulse curve, we assigned precise date intervals (Goodsite et al., 2001; Spalding et al., 2005). We then combined these calibrated ages with the 2 conventional radiocarbon ages, interpolating the dates for each depth using Clam age depth model (Figure S5 in Supporting Information S1) (Blaauw, 2010). The carbon accumulation rate for each peat layer (1 cm resolution) was computed using the age model, bulk density and carbon content. The long-term apparent rate of carbon accumulation (LORCA, $gCm^{-2}.yr^{-1}$) was derived by dividing the total mass of accumulated carbon by the deepest 14C calibrated age (Turunen, 2003). Recent apparent rates of carbon accumulation (RERCA; $gC.m^{-2}.yr^{-1}$) were calculated by dividing the total mass of carbon accumulated in the acrotelm by three ages (1850 CE, 1900 CE and 1950 CE) up to the coring year (2016 CE).

2.8. Net Ecosystem Carbon Balance

In order to assess the carbon dynamics of the peatland, the net annual ecosystem carbon balance (NECB) was computed for each year spanning 2017 to 2022. The NECB was determined as follows: $NECB = ER - GPP + FCH_4 + FDOC$, considering these variables as the primary sources and sinks within the peatland (Chapin et al., 2006). Loss of carbon by VOCs (volatile organic compounds) were not considered, as they could not be assessed. Regarding fluvial carbon export, dissolved CO_2, CH_4 and POC (particulate organic carbon) contribution, were not included due to lack of instrumentation In a previous study (Rosset et al., 2019), POC export had been estimated to represent 17% of the total organic fluvial export. Note that this sign convention is opposite to Chapin's original definition but simplifies the comparison with NEE. A negative value in the NECB signifies carbon uptake by the peatland, indicating its role as a carbon sink. We use modeled values for ER, GPP and FCH_4, and measured values for FDOC.

2.9. Uncertainties Estimation of the Models in the Annual Cumulated NEE and FCH_4

We established the models that fit best the observations for GPP, ER, NEE and CH_4 fluxes. To estimate the uncertainty related to this choice of models, we used the bootstrap function in the scipy.stats library to calculate "a two-sided bootstrap confidence interval of a statistic" (https://docs.scipy.org/doc/scipy/reference/generated/scipy.stats.bootstrap.html). This function first "takes a random sample of the original sample (with replacement)." Second, "Compute the bootstrap distribution of the statistic: for each set of resamples, compute the test statistic" and finally "Determine the confidence interval" δ. With this function, we have calculated the 95% confidence interval for the $coef_{director}$ coefficient of the linear regression between the best fit and the observations: $observations = coef_{director} \times bestfit$. Then by multiplying $coef_{director} \pm \delta$ (confidence interval) and the best fit time series, we obtain an estimate of the 95% confidence interval of the best fit of the GPP, ER, and CH_4 fluxes, and thus get an idea of the uncertainty of the models in relation to the observed data. To obtain the confidence interval of the NEE, the addition of the confidence interval of GPP and RE was used ($\delta_{NEE} = \delta_{GPP} + \delta_{RE}$).

3. Results

3.1. Environmental Variables

The mean annual temperature ranged between 7.72 and 9.39°C, with 2022 being the warmest year of the entire study (Table 1). The growing season in Bernadouze extends from mid-April to late October due to low

Table 1
Mean Annual Air Temperature (MAAT, °C), Precipitation (MAP, mm.year^{-1}), Flow of the Stream (mm), Range (Min-Max) for Annual DOC Export (gC m^{-2}.year^{-1}), and Cumulated GPP, ER, NEE, FCH$_4$ and NECB (gC m^{-2}.year^{-1}) From 2017 to 2022 and Associated Uncertainties

Year	2017	2018	2019	2020	2021	2022
MAAT °C	7.77	7.72	7.83	8.68	7.95	9.4
MAP (mm)	1,444	1,843	1,603	1,602	1,385	1,224
Flow (mm)	390	433	345	492	345	244
FDOC (gC.m^{-2}.year^{-1})	[15.9 − 21.2]	[14.5 − 19.3]	[17.9 − 23.9]	[31.2 − 41.6]	[16 − 21.3]	[13.4 − 17.2]
GPP (gC.m^{-2}.year^{-1})	645 ± 77	665 ± 79	556 ± 66	564 ± 67	615 ± 73	614 ± 73
ER (gC.m^{-2}.year^{-1})	622 ± 93	603 ± 90	634 ± 95	620 ± 93	599 ± 89	770 ± 115
NEE (gC.m^{-2}.year^{-1})	−23 ± 170	−62 ± 169	78 ± 161	56 ± 160	−16 ± 163	156 ± 188
FCH4 (gC.m^{-2}.year^{-1})	20.5 ± 3.5	21.8 ± 3.8	16.9 ± 2.9	19.4 ± 3.4	20.7 ± 3.6	18 ± 3.1
NECB (gC.m^{-2}.year^{-1})	15 ± 176	−23 ± 175	115 ± 167	111 ± 169	23 ± 169	189 ± 193

temperatures, limited light availability, and the regular presence of a snow cover. Annual accumulated precipitation ranged between 1,224 and 1,843 mm, with 2022 being the driest recorded year during the study (Table 1). The mean water table was −0.21 m below the soil surface during the entire measuring period, with slight mean WTD interannual variation (range −0.18 m to −0.25 m; Figure S3b in Supporting Information S1). A large decrease in the WTD was observed each year during summer, supported by a concomitant decrease in rainfall and an increase in air temperature. Specifically, the mean interannual WTD for July and August was −0.35 ± 0.13 m. However, in 2019 and 2022, the WTD during these months was down to −0.43 ± 0.11 m and −0.53 ± 0.10 m, respectively, compared to the four other years when the mean WTD stayed between −0.28 and −0.32 m.

3.2. Observed CO_2 and CH_4 Fluxes

Observed net ecosystem exchange (NEE), gross primary productivity (GPP), and ecosystem respiration (ER) exhibited clear seasonal variations throughout the years of measurements. Interannual variation was particularly pronounced for NEE, with peak measurements ranging from around −5 to around −12 μmol.m^{-2}.s^{-1} in 2020 and 2022, respectively. This pattern of NEE was likely driven by the interannual variation of peak GPP, whose lower and higher values were also observed in 2020 (14.9 ± 3.21 μmol.m^{-2}.s^{-1}) and in 2022 (21.3 ± 3.92 μmol.m^{-2}.s^{-1}), respectively. In contrast, interannual variations in ER fluxes were less clear, with peak values ranging from 9.77 ± 2.37 to 13.6 ± 1.23 μmol.m^{-2}.s^{-1}, with the largest flux observed in 2019. For methane (CH_4), stable emissions were observed throughout 2019, but a marked seasonal cycle was evident in the other three years, particularly in 2021 and 2022 (Figure 2d). Average CH_4 measurements over the four years of measurements were 52.9 ± 37.8 nmol.m^{-2}.s^{-1}. Finally, measurements of ER and CH_4 conducted with a snow cover on the peatland (>1m) during the 2021–2022 winter, averaged 0.64 ± 0.17 μmol.m^{-2}.s^{-1} and 22.8 ± 8.55 nmol.m^{-2}.s^{-1}, respectively (Figures 2c and 2d).

3.3. Modeled CO_2 and CH_4 Fluxes

The degree of correlation between the modeled values of GPP and ER and the measured ones, was evaluated using the R^2 of the Pearson correlation coefficient (Figure S7 in Supporting Information S1). The obtained R^2 values of 0.69 and 0.84 for GPP and ER, respectively, indicated a satisfactory performance of the models to represent the underlying CO_2 flux processes. However, for CH_4 and NEE the correlation between the modeled values and measured values is weaker, with R^2 values of 0.59 and 0.45.

3.4. Seasonal Evolution and Interannual Variability GPP, ER and NEE Fluxes

The annual cumulated GPP ranged from 556 to 665 gC.m^{-2}.yr^{-1} with a mean of 610 ± 39 gC.m^{-2}.yr^{-1} (Figure 4a). For ER, the annual cumulated value remained relatively consistent from 2017 to 2021, ranging from 599 to 634 gC.m^{-2}.yr^{-1}; however a notable increase of the annual cumulated ER of 22% was observed in 2022, reaching 770 gC.m^{-2}.yr^{-1} (Figure 4b). This interannual variability of GPP and ER resulted in very large differences in annual NEE, ranging from −62 gC.m^{-2}.yr^{-1} in 2018 to 156 gC.m^{-2}.yr^{-1} in 2022. These large

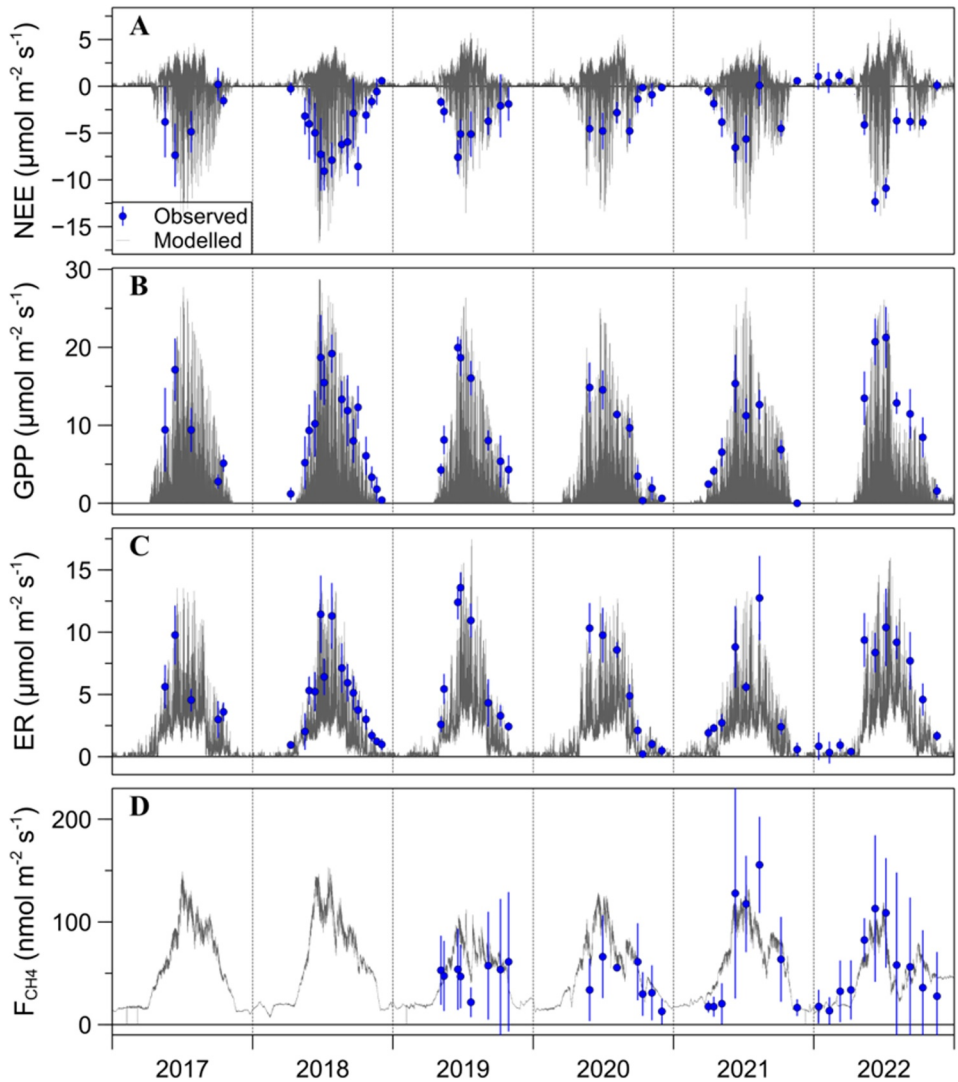

Figure 2. Observed (blue; mean ± SD, $n = 5$) and modeled (gray) (a) NEE (µmol.m^{-2}.s^{-1}), (b) GPP (µmol.m^{-2}.s^{-1}), (c) ER (µmol.m^{-2}.s^{-1}), and (d) FCH_4 (nmol.m^{-2}.s^{-1}) fluxes from January 2017 to December 2022 in the peatland of Bernadouze.

differences can be explained by the seasonal cycle of these fluxes and their cumulated values. During winter, from November to April, the peatland is covered in snow, resulting in zero GPP and low but constant ER, resulting in positive NEE. Then, starting from April, both GPP and ER increased significantly, producing a sharp increase in the cumulated values. During this period, the increase in NEE was faster (larger ER than GPP) in years 2017–2019 but remained stable from 2020 to 2022. This is related to a later start of photosynthesis in 2017–2019. Then, in early June, the cumulated NEE started to decrease, driven by an uptake of C by the peatland (GPP ≥ ER). For all years except 2017 and 2018, cumulated NEE increased again from mid-July to August or September, indicating lower GPP than ER. This mid-summer periods with lower GPP than ER corresponded to low levels of the WT in mid-summer in the last 4 years (Figure S3 in Supporting Information S1). This peak in the NEE value was specifically marked for 2019, 2020, and 2022, for which the system fully turned into a source of C, while it remained a C sink for the other years. After that, cumulated NEE decreased again due to higher GPP than ER until September (for 2019, 2020, and 2022) and October (for 2017, 2018, 2021).

Finally, uncertainties have been established for all fluxes and are presented in Figures S8 and S9 in Supporting Information S1. These allow us to take into account biases due to statistical modeling, as well as biases due to the spatialization of measurements on the peatland. Although the uncertainties associated with the cumulated fluxes are significant, the general trend remains the same.

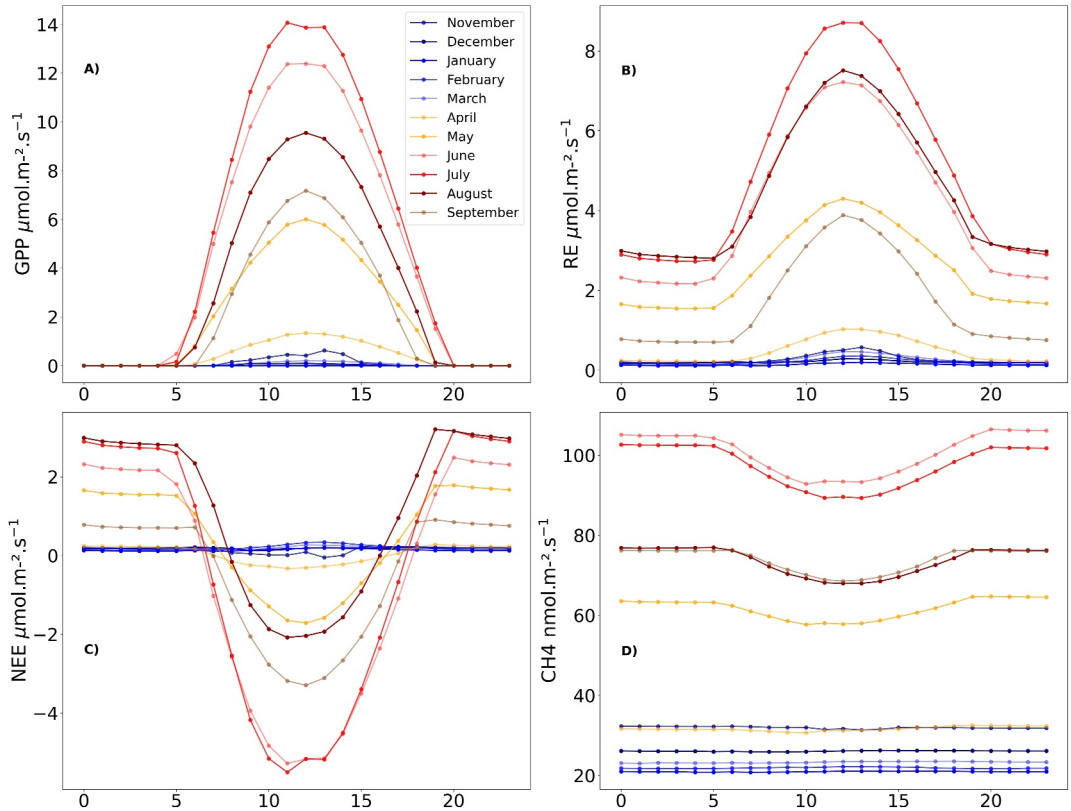

Figure 3. Monthly average diurnal cycle of modeled GPP, ER, NEE, and CH_4 over the 2017–2022 period.

3.5. Fluvial Organic Carbon Exports

The DOC export from the peatland exhibited a high interannual variability, with values ranging from [13.4–17.2] to [31.2–41.6] $gC.m^{-2}.yr^{-1}$ over the reported period (Table 1). The range provided here for the specific DOC flux covers the uncertainties related to the water inflow due to the karstic nature of the watershed (Rosset et al., 2019). For annual carbon balance, an annual mean value is considered.

3.6. Net Annual Ecosystem Carbon Balance

The peatland NECB showed a large interannual variability, ranging from −23 to 189 $gC.m^{-2}.yr^{-1}$ (mean of 55 $gC.m^{-2}.yr^{-1}$) (Figure 5). The peatland was a net source of C for all years except 2018. FCH_4 and FDOC fluxes constituted an equivalent contribution to NECB. Cumulated FCH_4 remained stable for all years with a mean value of 20 ± 1.7 $gC.m^{-2}.yr^{-1}$, which represented 36% of the mean NECB during the whole studied period. FDOC with an average value of 21.2 ± 7.1 $gC.m^{-2}.yr^{-1}$, accounted for 38% of mean NECB over the entire period.

3.7. Long Term Carbon Accumulation Rates

The analyzed peat core showed a high density of the peat below 10 cm depth, with a peak of 0.37 $g.cm^{-3}$ at 30 cm and an average value of 0.22 ± 0.06 $g.cm^{-3}$ for the whole core below 10 cm (Figure S6 in Supporting Information S1). The carbon content was consistently high and uniform along the entire core, with an average of 43.9 ± 2.6% C. A decrease of carbon content (down to 33% C) was observed around 30 cm, consistent with the increase of bulk density (Figure S6 in Supporting Information S1). The peat is dating back to 4088 Yr BP at a depth of 73 cm. The 14 C data are summarized in the Table S2 in Supporting Information S1. The LORCA was calculated at 16.4 $gC.m^{-2}.yr^{-1}$, while larger values were observed for RERCA, with 48.5, 59.2 and 72.1 $gC.m^{-2}.yr^{-1}$ since 1850 CE, 1900 CE and 1950 CE, respectively.

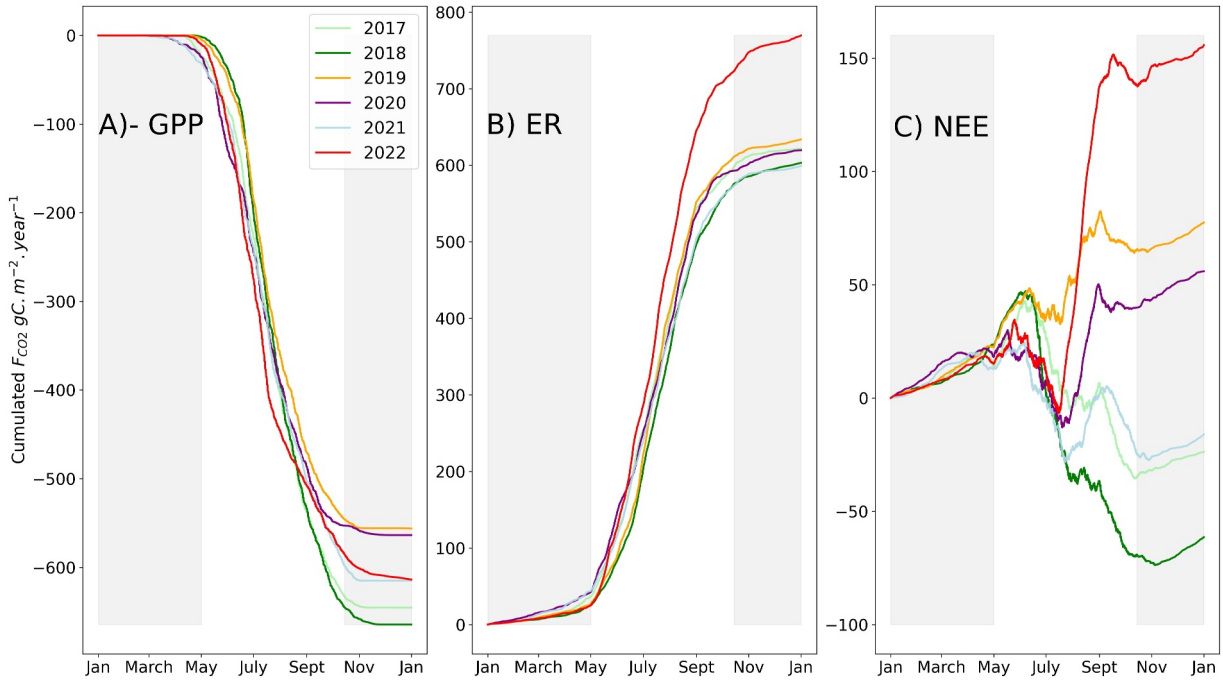

Figure 4. Cumulative values (gC.m^{-2}.yr^{-1}) of (a) -GPP, (b) ER and (c) NEE over the period 2017 to 2022. The shaded area correspond to the time periods when the peatland is covered with snow.

3.8. Combined Effect of AT and WTD on Annual Cumulated Fluxes

For the 2017–2021 period only, a strong correlation between the annual values of GPP, ER, NEE, FCH_4 and the Drought Index (DI) was evidenced (Figure 6). A rising drought index, that is, an increase in AT and/or a decrease in WTD, led to a reduction in GPP (Figure 6a). Conversely, this rise resulted in an increase in ER and NEE

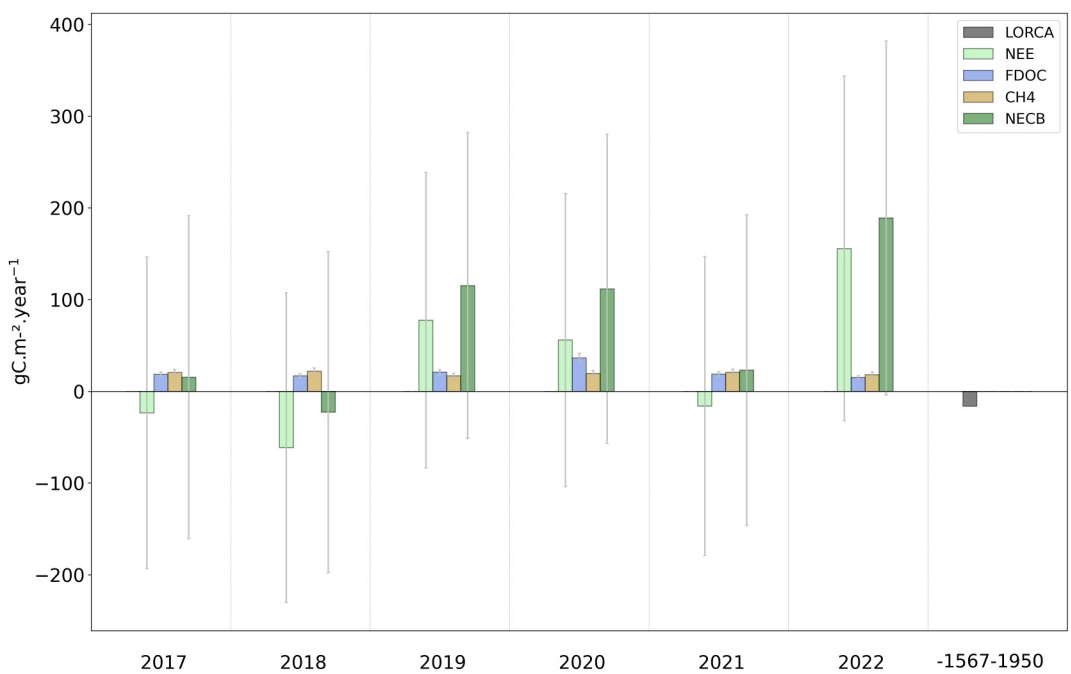

Figure 5. Annual values with uncertainties (in gray) of NEE, FCH_4, FDOC, and NECB between 2017 and 2022 (gC.m^{-2}.yr^{-1}), and LORCA (gC.m^{-2}.yr^{-1}).

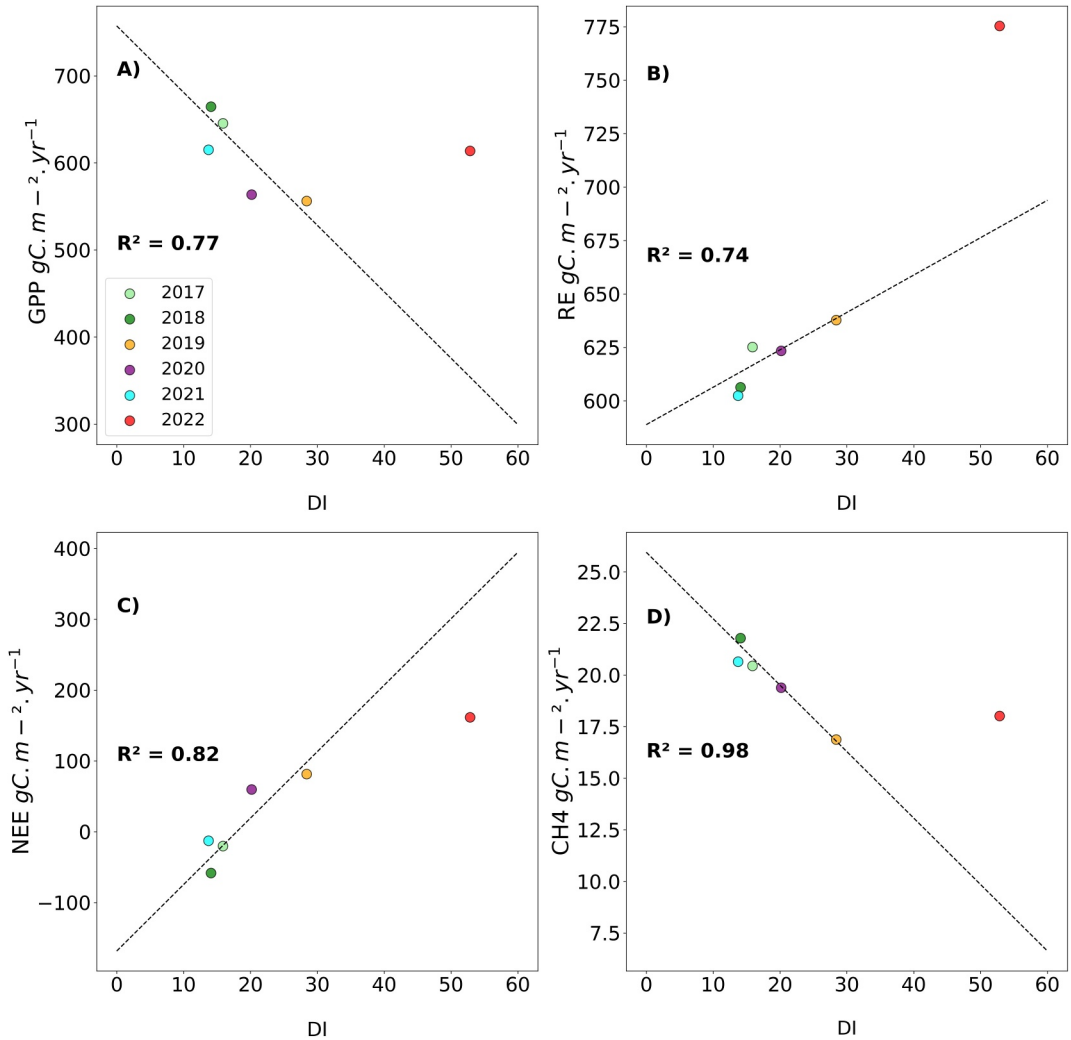

Figure 6. Relationships between annual cumulated values ($gCm^{-2}.year^{-1}$) of (a) GPP, (b) ER, (c) NEE, and (d) FCH_4 and the drought index DI. Black linear regression corresponds to the 2017–2021 period.

(Figures 6b and 6c). Additionally, a decrease in FCH_4 with increased DI could also be observed (Figure 6d). The year 2022 was characterized by a strong drought (DI value of 53). For this 2022, the annual carbon fluxes did not follow the linear regression established with DI for the preceding years (Figure 6).

4. Discussion

4.1. Fluxes Modeling Strategy: Benefits From Combining In Situ and Remote Sensing Data

The inclusion of the CI vegetation index to the GPP, CH_4 and indirectly ER flux models significantly improved their reliability (Table S3 in Supporting Information S1). Other studies have previously included satellite vegetation indices to model peatland GPP (Harris & Dash, 2011; Ingle et al., 2023; Junttila et al., 2021; Lees et al., 2021; Schubert et al., 2010) (see Equation 1). As presented by Gao et al. (2015) and again by Junttila et al. (2021), the inclusion of GPP in the respiration Equation 2 improved the ecosystem respiration model. This is because ecosystem respiration includes vegetation respiration that is on average proportional to GPP (see for instance Collalti and Prentice (2019)).

We chose to model NEE as the difference between ER and GPP instead of directly modeling NEE. Since our NEE measurements were all taken at midday, they were all negative (see Figure 2). As a result, direct modeling of NEE, even if it led to a stronger correlation coefficient ($R^2 = 0.69$), did not enable us to reconstruct meaningful diurnal

NEE fluxes. The separation between photosynthesis and respiration fluxes therefore appeared to be of prime importance to reproduce a positive NEE flux during the night and negative ones when photosynthesis exceeds respiration during the day (Figure 3) (D Acunha et al., 2019; Lafleur et al., 2001).

In our study, the chlorophyll index is key for CH_4 exchanges modeling. In particular, observed CH_4 fluxes correlated very well with the CI × PAR product at our site, enabling the reproduction of the diurnal cycle described by other studies (Lhosmot et al., 2022; Long et al., 2010). CH_4 fluxes are usually modeled using temperature and water table fluctuations (Baird et al., 2019). Only a limited number of studies have used vegetation indices (Rasanen et al., 2021; Sjogersten et al., 2023; Tucker et al., 2022). Our statistical CH_4 model shows higher nighttime than daytime CH_4 emissions (Figure 3). Recent publications on methane emissions from peatlands have highlighted the links observed between photosynthesis fluxes, PAR and methane fluxes to explain this observation. In particular, Lhosmot et al. (2022); Knox et al. (2021) showed that for temperate *Sphagnum* peatlands, diurnal methane fluxes reach their minimum when PAR and photosynthesis are at their maximum. In our model, The CI × AT product modulates the seasonality of CH_4 fluxes, the latter widely documented and linked to soil and air temperature (Chang, 2022; Chi et al., 2020).

This approach is promising in the perspective of studying carbon cycling in mountainous peatland sites where installation of EC tower is difficult if not impossible. Optical remote sensing can also serve to acquire spatialized proxies for peatland like plant biomass (Pang et al., 2023) or water table depth (Burdun et al., 2023) These proxies can then be utilized to derive spatialized carbon balances for peatlands, offering valuable data for broader-scale studies.

4.2. Beyond NEE: Contribution of Under-Studied Fluxes in Mountain Peatland NECB

While the NEE continues to be the primary factor influencing the NECB, our study revealed the relative importance, for a mountainous peatland site, of usually under-considered fluxes in peatland carbon studies, like winter CH_4 and fluvial organic carbon fluxes. CH_4 fluxes are in the high range of those reported by Abdalla et al. (2016) for northern peatlands. The annual cumulative CH_4 emissions represented 78% of total NEE emissions. If methane emissions are the highest during the summer, our study revealed that methane winter fluxes (when the peatland is covered with snow) accounted for 17% of annual methane emissions, whereas winter CO_2 fluxes accounted only for 5% of total respiration fluxes. Similar contributions (10%–30%) of winter fluxes to annual methane emissions had previously been reported for boreal peatlands (Dise, 1992; Pelletier et al., 2007; Strack et al., 2008; Webster et al., 2018) and mountain wetlands (Mast et al., 1998). Changes in winter fluxes have been shown to influence the annual carbon balance (Nugent et al., 2018). In addition to winter fluxes, our study of the carbon balance of the Bernadouze mountain peatland showed that fluvial carbon exports were crucial when estimating the ecosystem NECB. For the studied period (6 years), carbon export of fluvial organic carbon (127 $gC.m^{-2}$) was equivalent to the CH_4 emissions (117 $gC.m^{-2}$).

The annual DOC exports represented from 8% (2022) to 106% (2021) of NECB. When all years are combined, the fluvial organic carbon export represented 38% of the peatland carbon loss (NECB over 6 years). This proportion would even increase if POC was included. At this peatland, it could represent 17% of the fluvial carbon export (Rosset et al., 2019). The fluvial export represented 66% of the carbon emitted as CO_2 (NEE). This is more than what has been reported by Dinsmore et al. (2010) in Scotland, where DOC represented 24% of NEE C uptake and by Roulet et al. (2007) for the Mer Bleue peatland in Canada, where DOC represented on average 37% of mean NEE. This average value hides a strong interannual variability. In 2022, because of the drought, fluvial export (13–17 $gC.m^{-2}$) was small compared to carbon release as CO_2 (156 $gC.m^{-2}$). In contrast, in 2021, the fluvial export of carbon (16–21 $g.m^2$) was equivalent to the carbon uptake of CO_2 by the peatland (16 $g.m^2$) presumably attributed to the mountainous terrain, the peatland's relatively modest size in relation to the watershed, and episodes of heavy precipitation which tend to accentuate the contribution of fluvial exports (Rosset et al., 2019).

4.3. Temperate Mountain Peatlands: From Weak Carbon Sinks to Potential Carbon Sources

The Bernadouze peatland has been, on average, a modest carbon sink in the past millennium. The LORCA value reported for this site is lower than the average value reported for temperate peatlands, 26.1 ± 1.47 $gCm^{-2}.yr^{-1}$ (Charman et al., 2013), or more recently for several peatlands in central-Eastern Europe with an average of 21 $gCm^{-2}.yr^{-1}$ (Longman et al., 2021). This mountain peatland show similar LORCA to boreal peatlands, that exhibit values ranging from 13 to 35 $gCm^{-2}.yr^{-1}$ (Loisel et al., 2014; Loisel & Yu, 2013; Primeau &

Garneau, 2021; Ratcliffe et al., 2018; Turunen, 2003). In contrast to LORCA, the RERCA values for Bernadouze reveal much higher rates of C accumulation, ranging from 48.5 to 72.1 $gCm^{-2}.yr^{-1}$. However, the elevated values of C accumulation rates at the top of the core, as highlighted by Payne et al. (2019); Young et al. (2019) are due to the presence of undecomposed acrotelm peat, and underestimation of respiration fluxes. In contrast with the above results, our integrated study indicates that this peatland acted as a net source of carbon between 2017 and 2022, with an average positive NECB value of 55 $gCm^{-2}.yr^{-1}$. The few existing peatland NECB report mostly carbon sink, with a important interannual variability (Roulet et al., 2007). In Bernadouze, the annual NECB variability mainly resulted from the variation in the annual NEE, while both DOC and CH_4 fluxes remained relatively stable over the studied period. This is inline with the 6 years study at Mer Bleue (Roulet et al., 2007) and the synthesis of Carter et al. (2012) when comparing CO_2 and CH_4 fluxes. At our site, the positive average NEE of 32 $gCm^{-2}.yr^{-1}$, contrasts with most of the reported values for temperate peatlands in the literature ranging from 0 to −200 $gCm^{-2}.yr^{-1}$ (Alekseychik et al., 2021; Nugent et al., 2018; Peichl et al., 2014).

This discrepancy between long term and recent carbon balance for the Bernadouze peatland suggest that the peatland might turn from a long term sink to a source of C. However, the timing and processes behind such a switch, are uncertain. A change in the carbon balance of the peatland can be expected from the ongoing climate change. Mean annual temperatures in the peatland increased by 1° since the early 1960ies and maximum temperatures by 8°C for instance. Knowing the sensitivity of ecosystem respiration to temperature (Ben & Thompson, 2010; Sun et al., 2023), it is likely that the ER increased in the last 50 years. It has been observed that drier conditions in summer were associated with lower carbon uptake in Canadian boreal peatlands (McDonald et al., 2023). Similarly, higher temperatures also mean higher evapotranspiration that may reduce soil water content and deepen the water table even if the precipitation remain stable. This also tends to increase C release to the atmosphere by promoting oxic decomposition. However, higher temperatures and longer growing season will favors GPP. Our results for the last 6 years indicate that the balance between C release and uptake was more in favor of C release, whether directly to the atmosphere as CO_2 or CH_4, or to the river system as DOC.

4.4. Impact of a Severe Drought on a Mountain Peatland Carbon Balance

This study add to the few field studies that have explored the impacts of severe drought on peatlands (Sterk et al., 2023). Mesocosm studies have been conducted to compensate for this scarcity (Dieleman et al., 2015; X. Kang et al., 2018; Robroek et al., 2024; Sterk et al., 2023). While these are valuable initial approaches, they do not fully replicate in situ conditions, including the influence of topography, hydrology, and microhabitats, all of which can modify gas exchanges. The severity of the 2022 drought on the peatland, quantified by the drought index (DI), stands out from the interannual variability of the site, at least over the 2017–2021 period. Recent climate studies based on the observational record showed that the summer of 2022 was exceptional compared to the last 50 years (Serrano-Notivoli et al., 2023; van der Woude et al., 2023). Paleoclimatic reconstructions for the Central Pyrenees even show that this summer was likely the driest in the last 280 years and the hottest in the last 700 years (Serrano-Notivoli et al., 2023).

We observed the combination of higher temperatures and the significant drop in the water table, likely driven by intense soil water evaporation due to high vapor pressure deficit and a lack of precipitation, resulted in an extreme drought. It led to premature vegetation senescence, thereby shortening the growing season. *Sphagnum* mosses, lacking stomata, are particularly vulnerable to drought and heat wave compared to vascular plants since they cannot regulate their own water content (Bragazza, 2008). In Equation 2, the decline in the CI vegetation index is responsible for the decrease in GPP during the 2022 drought (Figure S10 in Supporting Information S1). At our site, simultaneously, rising air temperatures and high evaporation rates have caused the peat to desiccate, permitting oxygen to infiltrate the soil. This, in turn, promoted the decomposition and oxidation of organic matter, as observed by Kuiper et al. (2014); Fenner and Freeman (2011). While autotrophic respiration associated with GPP declined, heterotrophic respiration increased more significantly, leading to a rise in ecosystem respiration as described by Keane et al. (2021); Fenner and Freeman (2011). Some studies present contrasted findings regarding respiration's response to drought, which may differ from our observations in 2022. Some suggest that if soil water content drops too low, CO_2 producing bacteria are unable to break down organic matter because they require water for survival (E. Kang et al., 2022). Others propose that microorganisms exhibit stability in the face of drought, making GPP reduction the primary mechanism behind NEE destabilization (Yan et al., 2022). In any case, drought disrupted the peatland's carbon balance, as evidenced by the significant increase in NEE. Similar observations have been made in all other relevant studies (Keane et al., 2021; Sterk et al., 2023; Yan et al., 2022).

The years 2019 and 2022, which have a higher DI index compared to the others (specifically, 28 and 53), exhibit the lowest annual cumulated CH_4 fluxes (16.9 and 18 $gC.m^{-2}$). As reported in the literature (Perryman et al., 2023; Wu et al., 2020; X. Kang et al., 2018; Goodrich et al., 2017), soil drying, which allows oxygen to infiltrate and oxidize methane, reduced surface CH_4 flux sources. The effect is not as strong on annual DOC, although it can be noticed that the lowest exports are recorded in 2022, in relation to the reduction of the annual discharge.

5. Conclusions

This study provides an interannual NECB for a mountain peatland. It highlighted the importance of taking into account winter CH_4 fluxes and fluvial export of DOC when establishing annual carbon balance for these ecosystems. The study's novel approach, combining field flux measurements, chlorophyll index derived from satellite images and statistical modeling, improved the reliability of flux modeling for GPP, CH_4, and ER for remote sites. It provided a comprehensive understanding of CO_2 and CH_4 exchanges on an hourly timescale, describing diurnal cycles consistent with the literature and allowing a better prediction of carbon fluxes. If the LORCA reported an average carbon accumulation at our site over millennia, the 6 years NECB revealed that the peatland acted as a net source of carbon. However, this trend still needs confirmation over the longer term, as the peatland may currently be in an exceptionally dry state, not reflecting its behavior over longer timescales.

Our study focuses on carbon fluxes and their driving factors, particularly emphasizing their response during a severe drought in 2022. It underscores the pivotal role played by water availability, air temperature, and their interplay, represented by the drought index, in determining the net ecosystem carbon balance of the peatland. Mountain peatlands are likely to face exceptional climatic events in the future. Our record for the year 2022 stands out due to exceptionally severe drought conditions, might represent what will become non-exceptional years in the future. During this period, the peatland experienced a shortened growing season, primarily because of substantial water stress. Consequently, this disturbance disrupted the equilibrium between gross primary productivity and ecosystem respiration, causing net ecosystem exchange to shift toward becoming a carbon source.

This study opens up opportunities for longer-term investigations into the effects of extreme drought on peatlands. The next step would involve examining post-drought years to analyze the peatland's short-term response to a drought. As droughts are likely to occur more frequently in the future (Dai, 2013), they will have a lasting impact on peatland ecosystems. Questions about how plant communities will adapt and the carbon sequestration capacity of peatlands will become increasingly important.

Data Availability Statement

The data presented here are available at https://doi.org/10.5281/zenodo.10878083 (Garisoain, 2024). The S2M data set is freely available on the AERIS data center on the following https://doi.org/10.25326/37#v2020.2 (Vernay et al., 2023). The S2M data are provided by Meteo-France, CNRS, CNRM, Centre d'Etudes de la Neige, through AERIS.

Acknowledgments
This work is a contribution to the REPLIM-OPCC project and has been partially supported by the FEDER funds through the INTERREG V-A Spain-France-Andorra (POCTEFA 2014-2020-503 (REPLIM project, ref. EFA056/15)) and ANR-15-CE01-0008, Observatoire Homme-Milieu Pyrenees Haut Vicdessos - LABEX DRIIHM ANR-11-LABX0010. The carbon survey was undertaken in the framework of the "Service National d'Observation des Tourbières" (SNO-French Peatland Observatory), part of the research infrastructure OZCAR, accredited by the INSU/CNRS. The authors want to thank Bertrand Decharme for his kind support and advice. This work is dedicated to Didier Galop, who initiated the survey on the Bernadouze peatland.

References

Abdalla, M., Hastings, A., Truu, J., Espenberg, M., Mander, U., & Smith, P. (2016). Emissions of methane from northern peatlands: A review of management impacts and implications for future management options. *Ecology and Evolution*, *6*(19), 7080–7102. https://doi.org/10.1002/ece3.2469

Alekseychik, P., Korrensalo, A., Mammarella, I., Launiainen, S., Tuittila, E.-S., Korpela, I., & Vesala, T. (2021). Carbon balance of a Finnish bog: Temporal variability and limiting factors based on 6 years of eddy-covariance data. *Biogeosciences*, *18*(16), 4681–4704. https://doi.org/10.5194/bg-18-4681-2021

Amblar-Frances, M. P., Ramos-Calzado, P., Sanchis-Llado, J., Hernanz-Lazaro, A., Peral-Garcia, M. C., Navascues, B., et al. (2020). High resolution climate change projections for the Pyrenees region. *Advances in Science and Research*, *17*, 191–208. https://doi.org/10.5194/asr-17-191-2020

Aurela, M., Riutta, T., Laurila, T., Tuovinen, J.-P., Vesala, T., Tuittila, E.-S., et al. (2007). CO_2 exchange of a sedge fen in southern Finland-the impact of a drought period. *Tellus B: Chemical and Physical Meteorology*, *59*(5), 826–837. https://doi.org/10.1111/j.1600-0889.2007.00309.x

Baird, A., Green, S., Brown, E., & Dooling, G. (2019). Modelling time-integrated fluxes of CO_2 and CH_4 in peatlands: A review. *Mires & Peat*, *24*, 1–15. https://doi.org/10.19189/MaP.2019.DW.395

Ben, B.-L., & Thompson, A. (2010). Temperature-associated increases in the global soil respiration record. *Nature*, *464*(7288), 579–582. https://doi.org/10.1038/nature08930

Billett, M., Charman, D., Clark, J., Evans, C., Evans, M., Ostle, N., et al. (2010). Carbon balance of UK peatlands: Current state of knowledge and future research challenges. *Climate Research*, *45*, 13–29. https://doi.org/10.3354/cr00903

Birkel, C., Broder, T., & Biester, H. (2017). Nonlinear and threshold-dominated runoff generation controls DOC export in a small peat catchment. *Journal of Geophysical Research: Biogeosciences*, *122*(3), 498–513. https://doi.org/10.1002/2016JG003621

Blaauw, M. (2010). Methods and code for 'classical' age-modelling of radiocarbon sequences. *Quaternary Geochronology*, *5*(5), 512–518. https://doi.org/10.1016/j.quageo.2010.01.002

Bortoluzzi, E., Epron, D., Siegenthaler, A., Gilbert, D., & Buttler, A. (2006). Carbon balance of a European mountain bog at contrasting stages of regeneration. *New Phytologist*, *172*(4), 708–718. https://doi.org/10.1111/j.1469-8137.2006.01859.x

Bragazza, L. (2008). A climatic threshold triggers the die-off of peat mosses during an extreme heat wave. *Global Change Biology*, *14*(11), 2688–2695. https://doi.org/10.1111/j.1365-2486.2008.01699.x

Burdun, I., Bechtold, M., Aurela, M., De Lannoy, G., Desai, A. R., Humphreys, E., et al. (2023). Hidden becomes clear: Optical remote sensing of vegetation reveals water table dynamics in northern peatlands. *Remote Sensing of Environment*, *296*, 113736. https://doi.org/10.1016/j.rse.2023.113736

Carter, M. S., Larsen, K. S., Emmett, B., Estiarte, M., Field, C., Leith, I. D., et al. (2012). Synthesizing greenhouse gas fluxes across nine European peatlands and shrublands – Responses to climatic and environmental changes. *Biogeosciences*, *9*(10), 3739–3755. https://doi.org/10.5194/bg-9-3739-2012

Chang, K.-Y. (2022). Warming reshapes methane fluxes. *Nature Climate Change*, *12*(11), 971–972. https://doi.org/10.1038/s41558-022-01511-5

Chapin, F. S., Woodwell, G. M., Randerson, J. T., Rastetter, E. B., Lovett, G. M., Baldocchi, D. D., et al. (2006). Reconciling carbon-cycle concepts, terminology, and methods. *Ecosystems*, *9*(7), 1041–1050. https://doi.org/10.1007/s10021-005-0105-7

Charman, D. J., Beilman, D. W., Blaauw, M., Booth, R. K., Brewer, S., Chambers, F. M., et al. (2013). Climate-related changes in peatland carbon accumulation during the last millennium. *Biogeosciences*, *10*(2), 929–944. https://doi.org/10.5194/bg-10-929-2013

Chi, J., Nilsson, M. B., Laudon, H., Lindroth, A., Wallerman, J., Fransson, J. E. S., et al. (2020). The net landscape carbon balance—Integrating terrestrial and aquatic carbon fluxes in a managed boreal forest landscape in Sweden. *Global Change Biology*, *26*(4), 2353–2367. https://doi.org/10.1111/gcb.14983

Choler, P. (2023). Above-treeline ecosystems facing drought: Lessons from the 2022 European summer heat wave. *Biogeosciences*, *20*(20), 4259–4272. https://doi.org/10.5194/bg-20-4259-2023

Collalti, A., & Prentice, I. C. (2019). Is NPP proportional to GPP? Waring's hypothesis 20 years on. *Tree Physiology*, *39*(8), 1473–1483. https://doi.org/10.1093/treephys/tpz034

D Acunha, B., Morillas, L., Black, T. A., Christen, A., & Johnson, M. S. (2019). Net ecosystem carbon balance of a peat bog undergoing restoration: Integrating CO_2 and CH_4 fluxes from eddy covariance and aquatic evasion with DOC drainage fluxes. *Journal of Geophysical Research: Biogeosciences*, *124*(4), 884–901. https://doi.org/10.1029/2019JG005123

Dai, A. (2013). Increasing drought under global warming in observations and models. *Nature Climate Change*, *3*(1), 52–58. https://doi.org/10.1038/nclimate1633

D'Angelo, B., Leroy, F., Guimbaud, C., Jacotot, A., Zocatelli, R., Gogo, S., & Laggoun-Defarge, F. (2021). Carbon balance and spatial variability of CO_2 and CH_4 fluxes in a sphagnum-dominated peatland in a temperate climate. *Wetlands*, *41*(1), 5. https://doi.org/10.1007/s13157-021-01411-y

De Vleeschouwer, F., Chambers, F., & Swindles, G. (2010). Coring and sub-sampling of peatlands for palaeoenvironmental research. *Mires & Peat*, *7*, 10.

Dieleman, C. M., Branfireun, B. A., McLaughlin, J. W., & Lindo, Z. (2015). Climate change drives a shift in peatland ecosystem plant community: Implications for ecosystem function and stability. *Global Change Biology*, *21*(1), 388–395. https://doi.org/10.1111/gcb.12643

Dinsmore, K. J., Billett, M. F., Skiba, U. M., Rees, R. M., Drewer, J., & Helfter, C. (2010). Role of the aquatic pathway in the carbon and greenhouse gas budgets of a peatland catchment. *Global Change Biology*, *16*(10), 2750–2762. https://doi.org/10.1111/j.1365-2486.2009.02119.x

Dise, N. B. (1992). Winter fluxes of methane from Minnesota peatlands. *Biogeochemistry*, *17*(2), 71–83. https://doi.org/10.1007/BF00002641

Faranda, D., Pascale, S., & Bulut, B. (2023). Persistent anticyclonic conditions and climate change exacerbated the exceptional 2022 european-mediterranean drought. *Environmental Research Letters*, *18*(3). https://doi.org/10.1088/1748-9326/acbc37

Fenner, N., & Freeman, C. (2011). Drought-induced carbon loss in peatlands. *Nature Geoscience*, *4*(12), 895–900. https://doi.org/10.1038/ngeo1323

Fonseca, A., Santos, J., Padua, L., & Santos, M. (2023). Unveiling the future of relict Mediterranean mountain peatlands by integrating the potential response of ecological indicators with environmental suitability assessments. *Ecological Indicators*, *157*, 111206. https://doi.org/10.1016/j.ecolind.2023.111206

Gao, Y., Yu, G., Li, S., Yan, H., Zhu, X., Wang, Q., et al. (2015). A remote sensing model to estimate ecosystem respiration in Northern China and the Tibetan Plateau. *Ecological Modelling*, *304*, 34–43. https://doi.org/10.1016/j.ecolmodel.2015.03.001

Garisoain, R. (2024). In situ mean GPP, ER, CH_4 from 2017-01-01 to 2022-12-31 on the Bernadouze peatland and hourly temperature, water table depth, PAR, precipitation, sentinel-2 chlorophyll index [Dataset]. *Zenodo*. https://doi.org/10.5281/zenodo.10878083

Garisoain, R., Delire, C., Decharme, B., Ferrant, S., Granouillac, F., Payre-Suc, V., & Gandois, L. (2023). A study of dominant vegetation phenology in a sphagnum mountain peatland using in situ and Sentinel-2 observations. *Journal of Geophysical Research: Biogeosciences*, *128*(10), e2023JG007403. https://doi.org/10.1029/2023JG007403

Gitelson, A., & Merzlyak, M. N. (1994). Quantitative estimation of chlorophyll-a using reflectance spectra: Experiments with autumn chestnut and maple leaves. *Journal of Photochemistry and Photobiology B: Biology*, *22*(3), 247–252. https://doi.org/10.1016/1011-1344(93)06963-4

Gogo, S., Paroissien, J.-B., Laggoun-Defarge, F., Antoine, J.-M., Bernard-Jannin, L., Bertrand, G., et al. (2021). The information system of the French Peatland Observation Service: Service National d'Observation Tourbières – A valuable tool to assess the impact of global changes on the hydrology and biogeochemistry of temperate peatlands through long term monitoring. *Hydrological Processes*, *35*(6). https://doi.org/10.1002/hyp.14244

Goodrich, J. P., Campbell, D. I., & Schipper, L. A. (2017). Southern Hemisphere bog persists as a strong carbon sink during droughts. *Biogeosciences*, *14*(20), 4563–4576. https://doi.org/10.5194/bg-14-4563-2017

Goodsite, M. E., Rom, W., Heinemeier, J., Lange, T., Ooi, S., Appleby, P. G., et al. (2001). High-resolution AMS 14C dating of post-bomb peat archives of atmospheric pollutants. *Radiocarbon*, *43*(2B), 495–515. https://doi.org/10.1017/S0033822200041163

Gorham, E., Lehman, C., Dyke, A., Clymo, D., & Janssens, J. (2012). Long-term carbon sequestration in North American peatlands. *Quaternary Science Reviews*, *58*, 77–82. https://doi.org/10.1016/j.quascirev.2012.09.018

Harenda, K. M., Lamentowicz, M., Samson, M., & Chojnicki, B. H. (2018). The role of peatlands and their carbon storage function in the context of climate change. In T. Zielinski, I. Sagan, & W. Surosz (Eds.), *Interdisciplinary approaches for sustainable development goals: Economic growth, social inclusion and environmental protection* (pp. 169–187). Springer International Publishing. https://doi.org/10.1007/978-3-319-71788-3_12

Harris, A., & Dash, J. (2011). A new approach for estimating northern peatland gross primary productivity using a satellite-sensor-derived chlorophyll index. *Journal of Geophysical Research*, *116*(G4), G04002. https://doi.org/10.1029/2011JG001662

Heinemeyer, A., Di Bene, C., Lloyd, A. R., Tortorella, D., Baxter, R., Huntley, B., et al. (2011). Soil respiration: Implications of the plant-soil continuum and respiration chamber collar-insertion depth on measurement and modelling of soil CO_2 efflux rates in three ecosystems. *European Journal of Soil Science*, *62*(1), 82–94. https://doi.org/10.1111/j.1365-2389.2010.01331.x

Henry, E., Infante Sanchez, M., & Corriol, G. (2014). Tourbière de Bernadouze (Suc-et-Sentenac, 09). Expérimentation d'une cartographie fine des végétations (Tech. Rep.). *Conservatoire botanique national des Pyrénées et de Midi-Pyrénées, Bagnères de Bigorre*.

Ingle, R., Bhatnagar, S., Ghosh, B., Gill, L., Regan, S., Connolly, J., & Saunders, M. (2023). Development of hybrid models to estimate gross primary productivity at a near-natural peatland using Sentinel 2 data and a light use efficiency model. *Remote Sensing*, *15*(6), 1673. https://doi.org/10.3390/rs15061673

Jalut, G., Delibrias, G., Dagnac, J., Mardones, M., & Bouhours, M. (1982). A palaeoecological approach to the last 21,000 years in the pyrenees: The peat bog of Freychinede (alt. 1350 m, Ariege, South France). *Palaeogeography, Palaeoclimatology, Palaeoecology*, *40*(4), 321–359. https://doi.org/10.1016/0031-0182(82)90033-5

Jovani-Sancho, A. J., Cummins, T., & Byrne, K. A. (2017). Collar insertion depth effects on soil respiration in afforested peatlands. *Biology and Fertility of Soils*, *53*(6), 677–689. https://doi.org/10.1007/s00374-017-1210-4

Junttila, S., Kelly, J., Kljun, N., Aurela, M., Klemedtsson, L., Lohila, A., et al. (2021). Upscaling northern peatland CO_2 fluxes using satellite remote sensing data. *Remote Sensing*, *13*(4), 818. https://doi.org/10.3390/rs13040818

Kang, E., Li, Y., Zhang, X., Yan, Z., Zhang, W., Zhang, K., et al. (2022). Extreme drought decreases soil heterotrophic respiration but not methane flux by modifying the abundance of soil microbial functional groups in alpine peatland. *CATENA*, *212*, 106043. https://doi.org/10.1016/j.catena.2022.106043

Kang, X., Yan, L., Cui, L., Zhang, X., Hao, Y., Wu, H., et al. (2018). Reduced carbon dioxide sink and methane source under extreme drought condition in an alpine peatland. *Sustainability*, *10*(11), 4285. https://doi.org/10.3390/su10114285

Keane, J. B., Toet, S., Ineson, P., Weslien, P., Stockdale, J. E., & Klemedtsson, L. (2021). Carbon dioxide and methane flux response and recovery from drought in a hemiboreal ombrotrophic fen. *Frontiers in Earth Science*, *8*. https://doi.org/10.3389/feart.2020.562401

Kirschke, S., Bousquet, P., Ciais, P., Saunois, M., Canadell, J. G., Dlugokencky, E. J., et al. (2013). Three decades of global methane sources and sinks. *Nature Geoscience*, *6*(10), 813–823. https://doi.org/10.1038/ngeo1955

Klos, P. Z., Lucas, R. G., & Conklin, M. H. (2023). Influence of critical zone architecture and snowpack on streamflow generation processes: A mountain-Meadow headwater system in a Mediterranean climate. *Water Resources Research*, *59*(7), e2023WR034493. https://doi.org/10.1029/2023WR034493

Knox, S. H., Bansal, S., McNicol, G., Schafer, K., Sturtevant, C., Ueyama, M., et al. (2021). Identifying dominant environmental predictors of freshwater wetland methane fluxes across diurnal to seasonal time scales. *Global Change Biology*, *27*(15), 3582–3604. https://doi.org/10.1111/gcb.15661

Kuiper, J. J., Mooij, W. M., Bragazza, L., & Robroek, B. J. M. (2014). Plant functional types define magnitude of drought response in peatland CO_2 exchange. *Ecology*, *95*(1), 123–131. https://doi.org/10.1890/13-0270.1

Lafleur, P. M., Roulet, N. T., & Admiral, S. W. (2001). Annual cycle of CO_2 exchange at a bog peatland. *Journal of Geophysical Research*, *106*(D3), 3071–3081. https://doi.org/10.1029/2000JD900588

Lees, K. J., Khomik, M., Quaife, T., Clark, J. M., Hill, T., Klein, D., et al. (2021). Assessing the reliability of peatland GPP measurements by remote sensing: From plot to landscape scale. *Science of the Total Environment*, *766*, 142613. https://doi.org/10.1016/j.scitotenv.2020.142613

Leroy, F., Gogo, S., Guimbaud, C., Bernard-Jannin, L., Hu, Z., & Laggoun-Defarge, F. (2017). Vegetation composition controls temperature sensitivity of CO_2 and CH_4 emissions and DOC concentration in peatlands. *Soil Biology and Biochemistry*, *107*, 164–167. https://doi.org/10.1016/j.soilbio.2017.01.005

Lhosmot, A., Jacotot, A., Steinmann, M., Binet, P., Toussaint, M.-L., Gogo, S., et al. (2022). Biotic and abiotic control over diurnal CH_4 fluxes in a temperate transitional poor fen ecosystem. *Ecosystems*, *26*(5), 951–968. https://doi.org/10.1007/s10021-022-00809-x

Loisel, J., Gallego-Sala, A. V., Amesbury, M. J., Magnan, G., Anshari, G., Beilman, D. W., et al. (2021). Expert assessment of future vulnerability of the global peatland carbon sink. *Nature Climate Change*, *11*(1), 70–77. https://doi.org/10.1038/s41558-020-00944-0

Loisel, J., van Bellen, S., Pelletier, L., Talbot, J., Hugelius, G., Karran, D., et al. (2017). Insights and issues with estimating northern peatland carbon stocks and fluxes since the Last Glacial Maximum. *Earth-Science Reviews*, *165*, 59–80. https://doi.org/10.1016/j.earscirev.2016.12.001

Loisel, J., & Yu, Z. (2013). Holocene peatland carbon dynamics in Patagonia. *Quaternary Science Reviews*, *69*, 125–141. https://doi.org/10.1016/j.quascirev.2013.02.023

Loisel, J., Yu, Z., Beilman, D. W., Camill, P., Alm, J., Amesbury, M. J., et al. (2014). A database and synthesis of northern peatland soil properties and Holocene carbon and nitrogen accumulation. *The Holocene*, *24*(9), 1028–1042. https://doi.org/10.1177/0959683614538073

Long, K. D., Flanagan, L. B., & Cai, T. (2010). Diurnal and seasonal variation in methane emissions in a northern Canadian peatland measured by eddy covariance. *Global Change Biology*, *16*(9), 2420–2435. https://doi.org/10.1111/j.1365-2486.2009.02083.x

Longman, J., Veres, D., Haliuc, A., Finsinger, W., Ersek, V., Pascal, D., et al. (2021). Carbon accumulation rates of Holocene peatlands in central–eastern Europe document the driving role of human impact over the past 4000 years. *Climate of the Past*, *17*(6), 2633–2652. https://doi.org/10.5194/cp-17-2633-2021

Mast, M. A., Wickland, K. P., Striegl, R. T., & Clow, D. W. (1998). Winter fluxes of CO_2 and CH_4 from subalpine soils in Rocky Mountain National Park, Colorado. *Global Biogeochemical Cycles*, *12*(4), 607–620. https://doi.org/10.1029/98GB02313

McDonald, R. M., Moore, P. A., Helbig, M., & Waddington, J. M. (2023). Reduced net CO_2 uptake during dry summers in a boreal shield peatland. *Journal of Geophysical Research: Biogeosciences*, *128*(2), e2022JG006923. https://doi.org/10.1029/2022JG006923

Millar, D. J., Cooper, D. J., Dwire, K. A., Hubbard, R. M., & von Fischer, J. (2017). Mountain peatlands range from CO_2 sinks at high elevations to sources at low elevations: Implications for a changing climate. *Ecosystems*, *20*(2), 416–432. https://doi.org/10.1007/s10021-016-0034-7

Montanari, A., Nguyen, H., Rubinetti, S., Ceola, S., Galelli, S., Rubino, A., & Zanchettin, D. (2023). Why the 2022 Po River drought is the worst in the past two centuries. *Science Advances*, *9*(32), eadg8304. https://doi.org/10.1126/sciadv.adg8304

Muhr, J., Hohle, J., Otieno, D. O., & Borken, W. (2011). Manipulative lowering of the water table during summer does not affect CO_2 emissions and uptake in a fen in Germany. *Ecological Applications*, *21*(2), 391–401. https://doi.org/10.1890/09-1251.1

Nugent, K. A., Strachan, I. B., Strack, M., Roulet, N. T., & Rochefort, L. (2018). Multi-year net ecosystem carbon balance of a restored peatland reveals a return to carbon sink. *Global Change Biology*, *24*(12), 5751–5768. https://doi.org/10.1111/gcb.14449

Page, S., & Baird, A. (2016). Peatlands and global change: Response and resilience. *Annual Review of Environment and Resources*, *41*(1), 35–57. https://doi.org/10.1146/annurev-environ-110615-085520

Pang, Y., Rasanen, A., Juselius-Rajamaki, T., Aurela, M., Juutinen, S., Valiranta, M., & Virtanen, T. (2023). Upscaling field-measured seasonal ground vegetation patterns with Sentinel-2 images in boreal ecosystems. *International Journal of Remote Sensing*, *44*(14), 4239–4261. https://doi.org/10.1080/01431161.2023.2234093

Parish, F., Silvius, M., Reed, M., Stringer, L., Joosten, H., Suryadiputra, N., & Lin, C. (2007). Management of peatlands for biodiversity and climate change. In F. Parish, A. Sirin, D. Charman, H. Joosten, T. Minaeva, & M. Silvius (Eds.), *Assessment on peatlands, biodiversity and climate change* (pp. 9-1–9-23).

Pavelka, M., Acosta, M., Kiese, R., Altimir, N., Brummer, C., Crill, P., et al. (2018). Standardisation of chamber technique for CO_2, N_2O and CH_4 fluxes measurements from terrestrial ecosystems. *International Agrophysics*, *32*(4), 569–587. https://doi.org/10.1515/intag-2017-0045

Payne, R. J., Ring-Hrubesh, F., Rush, G., Sloan, T. J., Evans, C. D., & Mauquoy, D. (2019). Peatland initiation and carbon accumulation in the Falkland Islands. *Quaternary Science Reviews*, *212*, 213–218. https://doi.org/10.1016/j.quascirev.2019.03.022

Peichl, M., Oquist, M., Lofvenius, M. O., Ilstedt, U., Sagerfors, J., Grelle, A., et al. (2014). A 12-year record reveals pre-growing season temperature and water table level threshold effects on the net carbon dioxide exchange in a boreal fen. *Environmental Research Letters*, *9*(5), 055006. https://doi.org/10.1088/1748-9326/9/5/055006

Pelletier, L., Moore, T. R., Roulet, N. T., Garneau, M., & Beaulieu-Audy, V. (2007). Methane fluxes from three peatlands in the La Grande Rivière watershed, James Bay lowland, Canada. *Journal of Geophysical Research*, *112*(G1), G01018. https://doi.org/10.1029/2006JG000216

Perryman, C. R., McCalley, C. K., Shorter, J. H., Perry, A. L., White, N., Dziurzynski, A., & Varner, R. K. (2023). Effect of drought and heavy precipitation on CH_4 emissions and $\delta^{13}C$–CH_4 in a northern temperate peatland. *Ecosystems*, *27*(1), 1–18. https://doi.org/10.1007/s10021-023-00868-8

Primeau, G., & Garneau, M. (2021). Carbon accumulation in peatlands along a boreal to subarctic transect in eastern Canada. *The Holocene*, *31*(5), 858–869. https://doi.org/10.1177/0959683620988031

Pullens, J. W. M., Sottocornola, M., Kiely, G., Toscano, P., & Gianelle, D. (2016). Carbon fluxes of an alpine peatland in Northern Italy. *Agricultural and Forest Meteorology*, *220*, 69–82. https://doi.org/10.1016/j.agrformet.2016.01.012

Ramirez, J. A., Baird, A. J., & Coulthard, T. J. (2017). The effect of sampling effort on estimates of methane ebullition from peat. *Water Resources Research*, *53*(5), 4158–4168. https://doi.org/10.1002/2017WR020428

Rasanen, A., Manninen, T., Korkiakoski, M., Lohila, A., & Virtanen, T. (2021). Predicting catchment-scale methane fluxes with multi-source remote sensing. *Landscape Ecology*, *36*(4), 1177–1195. https://doi.org/10.1007/s10980-021-01194-x

Ratcliffe, J., Payne, R., Sloan, T., Smith, B., Waldron, S., Mauquoy, D., et al. (2018). Holocene carbon accumulation in the peatlands of northern Scotland. *Mires & Peat*, *23*, 1–30. https://doi.org/10.19189/MaP.2018.OMB.347

Reille, M. (1990). The peat-bog of La Borde (eastern Pyrenees, France): A key site for the study of the Lateglacial in southern France. La tourbiere de La Borde (Pyrenees orientales, France): Un site de pour l'etude du Tardiglaciaire sud-europeen. *Comptes Rendus de l'Academie des Sciences, Serie 2; (France)*, *310*, 6.

Robroek, B. J. M., Devilee, G., Telgenkamp, Y., Harlin, C., Steele, M. N., Barel, J. M., & Lamers, L. P. M. (2024). More is not always better: Peat moss mixtures slightly enhance peatland stability. *Proceedings of the Royal Society B: Biological Sciences*, *291*(2014), 20232622. https://doi.org/10.1098/rspb.2023.2622

Rogora, M., Frate, L., Carranza, M. L., Freppaz, M., Stanisci, A., Bertani, I., et al. (2018). Assessment of climate change effects on mountain ecosystems through a cross-site analysis in the Alps and Apennines. *Science of the Total Environment*, *624*, 1429–1442. https://doi.org/10.1016/j.scitotenv.2017.12.155

Rosset, T., Binet, S., Antoine, J.-M., Lerigoleur, E., Rigal, F., & Gandois, L. (2020). Drivers of seasonal- and event-scale DOC dynamics at the outlet of mountainous peatlands revealed by high-frequency monitoring. *Biogeosciences*, *17*(13), 3705–3722. https://doi.org/10.5194/bg-17-3705-2020

Rosset, T., Binet, S., Rigal, F., & Gandois, L. (2022). Peatland dissolved organic carbon export to surface waters: Global significance and effects of anthropogenic disturbance. *Geophysical Research Letters*, *49*(5), e2021GL096616. https://doi.org/10.1029/2021GL096616

Rosset, T., Gandois, L., Le Roux, G., Teisserenc, R., Durantez Jimenez, P., Camboulive, T., & Binet, S. (2019). Peatland contribution to stream organic carbon exports from a montane watershed. *Journal of Geophysical Research: Biogeosciences*, *124*(11), 3448–3464. https://doi.org/10.1029/2019JG005142

Roulet, N. T., Lafleur, P. M., Richard, P. J. H., Moore, T. R., Humphreys, E. R., & Bubier, J. (2007). Contemporary carbon balance and late Holocene carbon accumulation in a northern peatland. *Global Change Biology*, *13*(2), 397–411. https://doi.org/10.1111/j.1365-2486.2006.01292.x

Rubel, F., Brugger, K., Haslinger, K., & Auer, I. (2017). The climate of the European Alps: Shift of very high resolution Koppen-Geiger climate zones 1800–2100. *Meteorologische Zeitschrift*, *26*(2), 115–125. https://doi.org/10.1127/metz/2016/0816

Santoni, S., Garel, E., Gillon, M., Babic, M., Spangenberg, J. E., Bomou, B., et al. (2023). The role of groundwater in CO_2 production and carbon storage in Mediterranean peatlands: An isotope geochemistry approach. *Science of the Total Environment*, *866*, 161098. https://doi.org/10.1016/j.scitotenv.2022.161098

Schubert, P., Eklundh, L., Lund, M., & Nilsson, M. (2010). Estimating northern peatland CO_2 exchange from MODIS time series data. *Remote Sensing of Environment*, *114*(6), 1178–1189. https://doi.org/10.1016/j.rse.2010.01.005

Serrano-Notivoli, R., Tejedor, E., Sarricolea, P., Meseguer-Ruiz, O., de Luis, M., Saz, M. A., et al. (2023). Unprecedented warmth: A look at Spain's exceptional summer of 2022. *Atmospheric Research*, *293*, 106931. https://doi.org/10.1016/j.atmosres.2023.106931

Sjogersten, S., Ledger, M., Siewert, M., de la Barreda-Bautista, B., Sowter, A., Gee, D., et al. (2023). Capabilities of optical and radar Earth observation data for up-scaling methane emissions linked to subsidence and permafrost degradation in sub-Arctic peatlands. *Biogeosciences Discussions* (pp. 1–30). https://doi.org/10.5194/bg-2023-17

Spalding, K. L., Buchholz, B. A., Bergman, L.-E., Druid, H., & Frisen, J. (2005). Age written in teeth by nuclear tests. *Nature*, *437*(7057), 333–334. https://doi.org/10.1038/437333a

Sterk, H. P., Marshall, C., Cowie, N. R., Clutterbuck, B., McIlvenny, J., & Andersen, R. (2023). Blanket bog CO_2 flux driven by plant functional type during summer drought. *Ecohydrology*, *16*(2), e2503. https://doi.org/10.1002/eco.2503

Strack, M., Waddington, J. M., Bourbonniere, R. A., Buckton, E. L., Shaw, K., Whittington, P., & Price, J. S. (2008). Effect of water table drawdown on peatland dissolved organic carbon export and dynamics. *Hydrological Processes*, *22*(17), 3373–3385. https://doi.org/10.1002/hyp.6931

Sun, W., Luo, X., Fang, Y., Shiga, Y. P., Zhang, Y., Fisher, J. B., et al. (2023). Biome-scale temperature sensitivity of ecosystem respiration revealed by atmospheric CO_2 observations. *Nature Ecology & Evolution*, *7*(8), 1199–1210. https://doi.org/10.1038/s41559-023-02093-x

Tucker, C., O'Neill, A., Meingast, K., Bourgeau-Chavez, L., Lilleskov, E., & Kane, E. S. (2022). Spectral indices of vegetation condition and soil water content reflect controls on CH_4 and CO_2 exchange in sphagnum-dominated northern peatlands. *Journal of Geophysical Research: Biogeosciences*, *127*(7), e2021JG006486. https://doi.org/10.1029/2021JG006486

Tunaley, C., Tetzlaff, D., & Soulsby, C. (2017). Scaling effects of riparian peatlands on stable isotopes in runoff and DOC mobilisation. *Journal of Hydrology*, *549*, 220–235. https://doi.org/10.1016/j.jhydrol.2017.03.056

Turetsky, M., Wieder, K., Halsey, L., & Vitt, D. (2002). Current disturbance and the diminishing peatland carbon sink. *Geophysical Research Letters*, *29*(11), 21-1–21-4. https://doi.org/10.1029/2001GL014000

Turetsky, M. R., Kotowska, A., Bubier, J., Dise, N. B., Crill, P., Hornibrook, E. R. C., et al. (2014). A synthesis of methane emissions from 71 northern, temperate, and subtropical wetlands. *Global Change Biology*, *20*(7), 2183–2197. https://doi.org/10.1111/gcb.12580

Turunen, J. (2003). Past and present carbon accumulation in undisturbed boreal and subarctic mires: A review. *Suo*, *54*, 15–28.

van der Woude, A. M., Peters, W., Joetzjer, E., Lafont, S., Koren, G., Ciais, P., et al. (2023). Temperature extremes of 2022 reduced carbon uptake by forests in Europe. *Nature Communications*, *14*(1), 6218. https://doi.org/10.1038/s41467-023-41851-0

Vernay, M., Lafaysse, M., & Hagenmuller, P. (2023). The S2M meteorological and snow cover reanalysis in the French mountainous areas (1958 - Present) [Dataset]. *Aeris*. https://doi.org/10.25326/37#v2020.2

Vernay, M., Lafaysse, M., Monteiro, D., Hagenmuller, P., Nheili, R., Samacoits, R., et al. (2022). The S2M meteorological and snow cover reanalysis over the French mountainous areas: Description and evaluation (1958–2021). *Earth System Science Data*, *14*(4), 1707–1733. https://doi.org/10.5194/essd-14-1707-2022

Vidal, J.-P., Martin, E., Franchisteguy, L., Baillon, M., & Soubeyroux, J.-M. (2010). A 50-year high-resolution atmospheric reanalysis over France with the Safran system. *International Journal of Climatology*, *30*(11), 1627–1644. https://doi.org/10.1002/joc.2003

Wang, H., Richardson, C. J., & Ho, M. (2015). Dual controls on carbon loss during drought in peatlands. *Nature Climate Change*, *5*(6), 584–587. https://doi.org/10.1038/nclimate2643

Webster, K. L., Bhatti, J. S., Thompson, D. K., Nelson, S. A., Shaw, C. H., Bona, K. A., et al. (2018). Spatially-integrated estimates of net ecosystem exchange and methane fluxes from Canadian peatlands. *Carbon Balance and Management*, *13*(1), 16. https://doi.org/10.1186/s13021-018-0105-5

Wu, H., Yan, L., Li, Y., Zhang, K., Hao, Y., Wang, J., et al. (2020). Drought-induced reduction in methane fluxes and its hydrothermal sensitivity in alpine peatland. *PeerJ*, *8*, e8874. https://doi.org/10.7717/peerj.8874

Xu, J., Morris, P. J., Liu, J., & Holden, J. (2018). PEATMAP: Refining estimates of global peatland distribution based on a meta-analysis. *CATENA*, *160*, 134–140. https://doi.org/10.1016/j.catena.2017.09.010

Yan, Z., Kang, E., Zhang, K., Hao, Y., Wang, X., Li, Y., et al. (2022). Asynchronous responses of microbial CAZymes genes and the net CO_2 exchange in alpine peatland following 5 years of continuous extreme drought events. *ISME Communications*, *2*(1), 1–12. https://doi.org/10.1038/s43705-022-00200-w

Yao, H., Peng, H., Hong, B., Guo, Q., Ding, H., Hong, Y., et al. (2022). Environmental controls on multi-scale dynamics of net carbon dioxide exchange from an alpine peatland on the eastern Qinghai-Tibet Plateau. *Frontiers in Plant Science*, *12*. https://doi.org/10.3389/fpls.2021.791343

Young, D. M., Baird, A. J., Charman, D. J., Evans, C. D., Gallego-Sala, A. V., Gill, P. J., et al. (2019). Misinterpreting carbon accumulation rates in records from near-surface peat. *Scientific Reports*, *9*(1), 17939. https://doi.org/10.1038/s41598-019-53879-8

Yu, Z. C. (2012). Northern peatland carbon stocks and dynamics: A review. *Biogeosciences*, *9*(10), 4071–4085. https://doi.org/10.5194/bg-9-4071-2012